Deletion of the potassium channel Kv12.2 causes hippocampal hyperexcitability and epilepsy

Xiaofei Zhang, Federica Bertaso, Jong W. Yoo, Karsten Baumgärtel, Sinead M. Clancy, Van Lee, Cynthia Cienfuegos, Carly Wilmot, Jacqueline Avis, Truc Hunyh, Catherine Daguia, Christian Schmedt, Jeffrey Noebels & Timothy Jegla

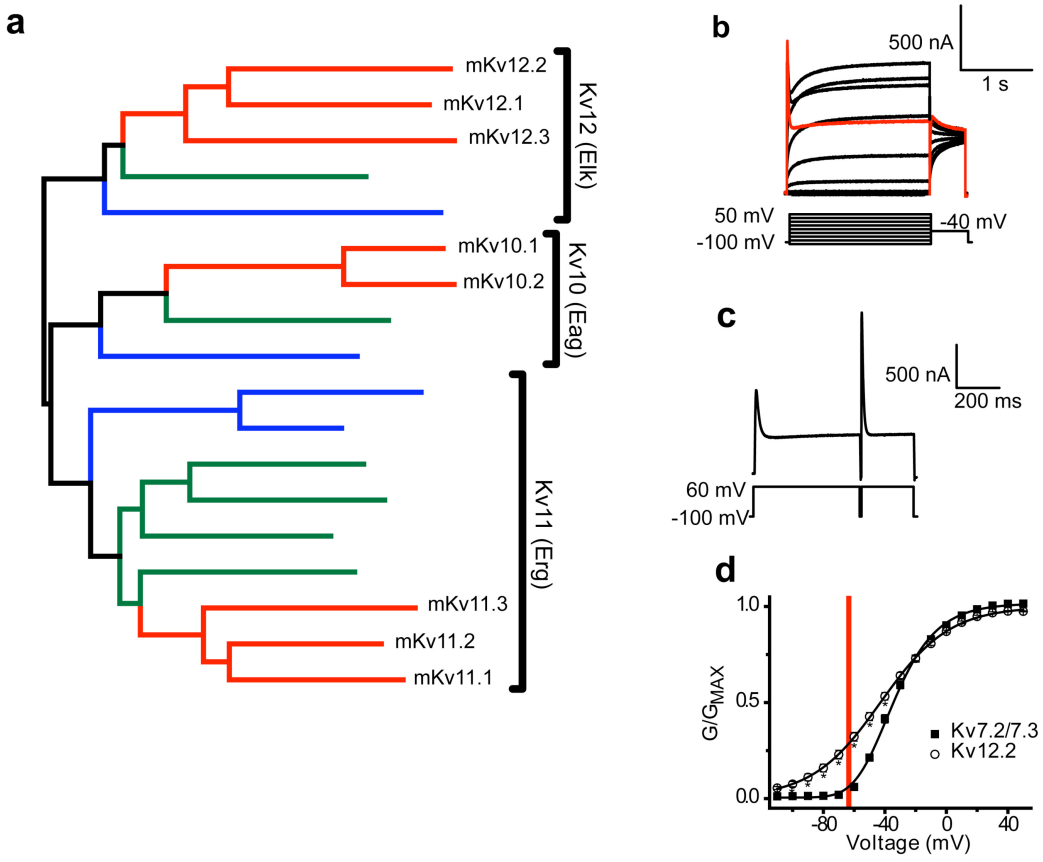

Supplementary Figure 1 | Evolution and biophysics of Kv12.2. (**a**) A Phylogeny of the *Ether–a–go–go* (EAG) K^+ channel superfamily shows three ancient conserved gene families, Elk (Kv12), Eag (Kv10) and Erg (Kv11). Mouse sequences (m, red) are given with IUPHAR names[1]. Sequences from *Nematostella* (green) and *Trichoplax* (blue) demonstrate subfamily conservation

Nature Neuroscience: doi:10.1038/nn.2610

throughout metazoan evolution. The Kv12 family gene expansion that includes *Kv12.2* (*KCNH3*) is vertebrate–specific. (**b**) Currents recorded in response to 2 s voltage steps from –110 mV to +50 mV (red) from *Xenopus* oocytes expressing Kv12.2. (**c**) Fast recovery from inactivation by Kv12.2 during a 5 ms repolarization to –100 mV interrupting a pulse to +60 mV. (**d**) Normalized conductance–voltage curves derived from tail currents and fit with a single Boltzmann (line) for Kv12.2 ($n = 6$) and Kv7.2/Kv7.3 (M–current, $n = 5$) expressed in oocytes. The red line shows the mean resting membrane potential of cultured WT hippocampal neurons (see **Fig. 2**); bars show s.e.m., and asterisks indicate significant difference ($p < 0.05$). The hyperpolarized activation range and rapid recovery from partial inactivation of Kv12.2 allow the channel to provide a steady–state K^+ current in the sub–threshold voltage range.

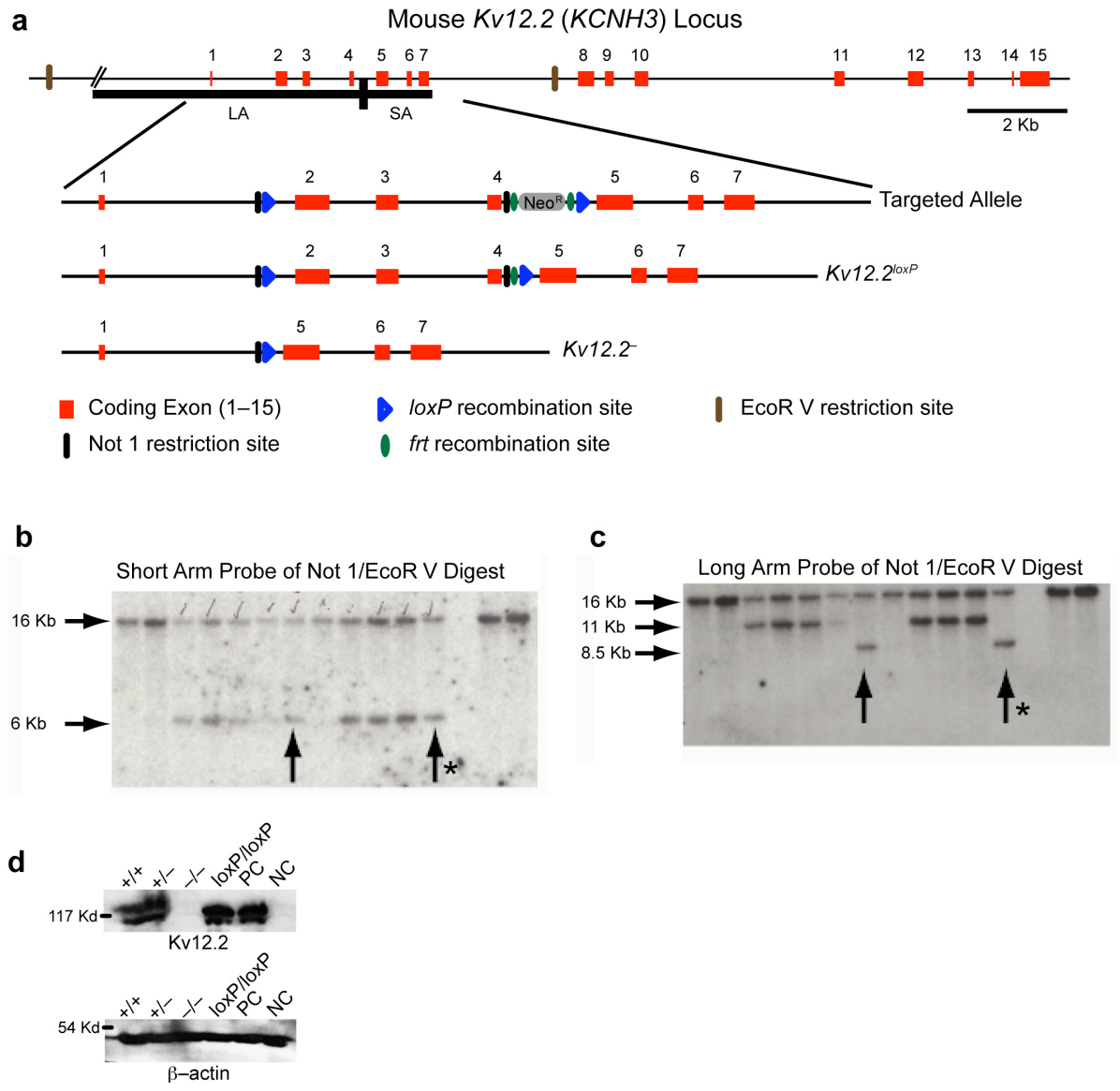

Supplementary Figure 2 | Conditional targeting strategy for genetic deletion of Kv12.2 in mice. (**a**) Map of the *Kv12.2* locus and blow up maps of the region targeted for deletion through homologous recombination. Coding exons are labelled 1–15 and native EcoR V restriction sites used in genotyping are indicated. Targeting of the mouse *Kv12.2* locus involved placing a neomycin resistance cassette (*Neo*^{R}) cassette (bracketed by *frt* recombination sites) between the 4th and 5th exons and *loxP* recombination sites surrounding this cassette and coding exons 2–4.

We bracketed the *Neo*^{R} cassette with *frt* sites for deletion by Flp–recombinase to produce a floxed allele (*Kv12.2*^{loxP}). Following excision with Cre recombinase, the deleted allele expresses only a truncated 25 amino acid protein off exon 1. The N–terminus of Kv12.2 has no effect on channel expression (data not shown) and this deleted allele therefore functions as a true null. Long and short homology arms of the targeting vector (LA and SA) are indicated with a bold black line under the *Kv12.2* locus map. Not 1 sites were placed in the targeting vector next to the *loxP* site in the first intron and at the 5' margin of the *Neo*^{R} cassette. The targeting vector also included dual negative selection cassettes bracketing the homology arms (diphtheria toxin, and thymidine kinase, not shown) to aid in selection of homologous recombinant cells. We transfected Bruce4 mouse ES cells with the linearized targeting construct and placed them under triple selection for G418 resistance, DTA synthesis and gancyclovir susceptibility. We isolated > 100 resistant cell colonies after 10–12 days of selection and screened them for homologous recombination in the short arm by PCR. (**b,c**) We screened positive clones to confirm proper recombination in both homology arms by standard Southern Blot analysis of genomic DNA cut with EcoR V and Not 1 using P^{32}–labelled probes located between the EcoR V sites and the targeting vector homology arms. Both probes hybridize to a ~16 Kb band EcoR V band in the *Kv12.2*$^{+}$ allele. Two ES cell lines carrying properly targeted alleles (arrows) have an additional ~5 Kb band labelled with the short arm probe (**b**) and an additional ~8.5 Kb labelled with the long arm probe (**c**), created by the insertion of Not 1 restriction sites in a single allele. ES cell lines missing the upstream *loxP* site also lack the adjacent Not 1 site and label an ~11 Kb band with the long arm probe. The ES cell line used to generate the *Kv12.2*$^{loxP/loxP}$ and *Kv12.2*$^{-/-}$ mouse lines is indicated with an asterisk. (**d**) Western blot of whole brain lysates confirming deletion of Kv12.2 protein from *Kv12.2*$^{-/-}$ neurons. *Kv12.2*$^{loxP/loxP}$ mice express normal Kv12.2 protein

levels. GAPDH and β–actin are loading controls. Controls lysates: CHO cells transfected with Kv12.2 (PC) or untransfected (NC).

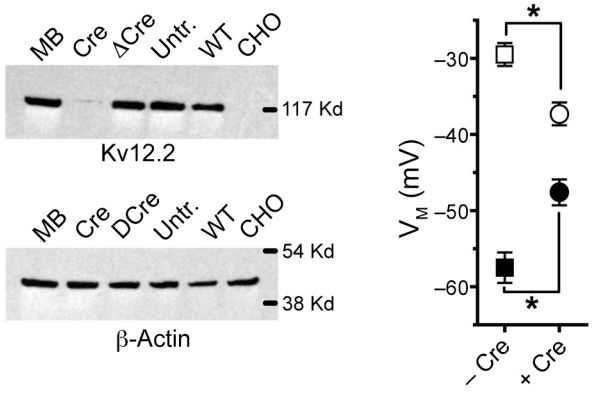

Supplementary Figure 3 | Conditional genetic deletion of Kv12.2 from cultured hippocampal pyramidal neurons results in hyperexcitability. (**a**) Western blot of Kv12.2 protein expression in cultured hippocampal pyramidal neurons from *Kv12.2*$^{loxP/loxP}$ mice infected with lentiviruses expressing a native Cre–recombinase/GFP fusion protein (Cre) or a truncated non–functional Cre–recombinase/GFP (ΔCre). Cre recombinase expression almost completely eliminated Kv12.2 protein. We used whole mouse brain lysate, uninfected *Kv12.2*$^{loxP/loxP}$ (untr.) and *Kv12.2*$^{+/+}$ hippocampal neurons as positive controls and untransfected Chinese Hamster Ovary (CHO) as a negative control. Blots were reprobed with an antibody to β–actin as a control for equal protein loading (bottom panel). (**b**) Resting potentials (closed symbols, n = 22–35) and action potential thresholds (open symbols, n = 28–35) for *Kv12.2*$^{loxP/loxP}$ neurons infected with Cre/GFP (+ Cre) or ΔCre/GFP (– Cre) lentivirus. Resting potential was significantly depolarized and action potential threshold was significantly hyperpolarized following Cre/GFP expression.

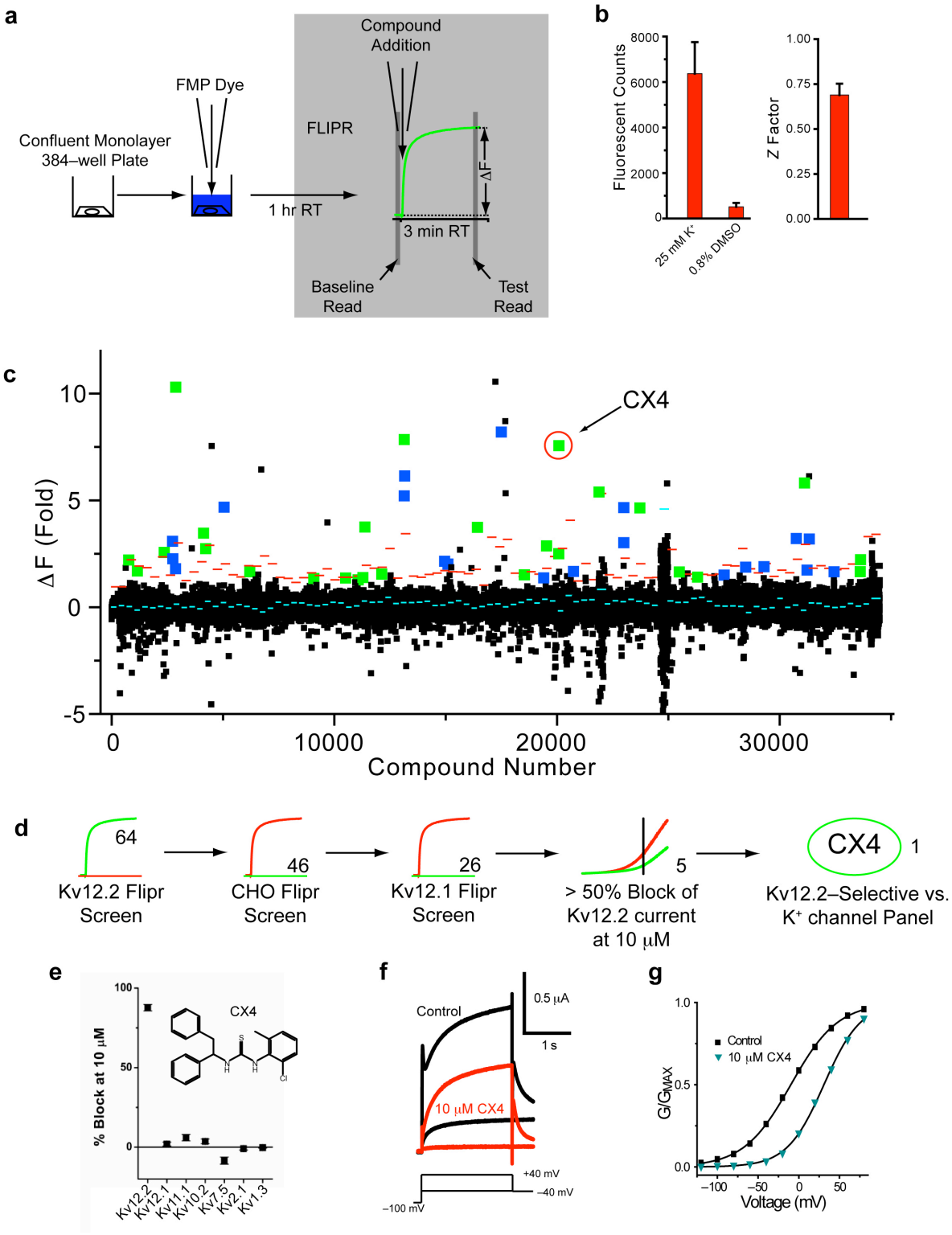

Supplementary Figure 4 | High throughput identification of a specific Kv12.2 inhibitor. We based a high throughput screen for Kv12.2 inhibitors on the observation that Kv12.2 strongly

hyperpolarizes the resting potential of Chinese Hamster Ovary (CHO) cells (data not shown), allowing channel block to be detected as membrane depolarization. (**a**) Screening assay procedure for Kv12.2 inhibitors. We plated CHO cells expressing human Kv12.2 under the control of a Tet–inducible promoter at a density of 8,000 cells/well in 384–well plates and induced them to express Kv12.2 overnight with 1 μg/ml tetracycline. Media was aspirated and replaced with 25 μl/well FMP dye (Molecular Devices, Sunnyvale, CA) for fluorescence–based detection of membrane potential. Following 1 hr incubation at room temperature, we transferred plates into a FLIPR 2 plate reader (Molecular Devices, Sunnyvale, CA). We read baseline fluorescence signals for 20 s, at which point test compounds were added in a 10 μl volume to a final concentration of 8 μM. Compound stocks contained DMSO and final DMSO concentration was 0.8%. We observed no effect of this DMSO concentration in the assay but nevertheless included it in negative controls. We read fluorescence signals 3 min after compound addition, and ΔF for each well was calculated as this read value minus the baseline read value. Depolarization was detected as a time–dependent increase in fluorescence following compound addition; positive controls of 25 mM K^+ included on each plate showed robust depolarization signals independent of Kv12.2 block. We screened 34,496 chemically diverse small molecules purchased from vendors in 98 384–well plates (352 compounds/plate plus positive (25 mM K^+) and negative (0.8% DMSO) controls). (**b**) Mean control values for the 98 plates (left) and mean *Z* factor for each plate (right); bars show s.e.m. *Z* factors > 0.5 indicate a robust assay[2], suggesting that the Kv12.2 assay should reliably detect compound–induced depolarizations. (**c**) Screening results for each test compound (squares) plotted as fold ΔF relative to negative controls. We calculated values separately for each plate using only controls (n = 8) from that plate. Cyan lines show ΔF for negative controls from each plate and red lines show 5 standard

deviations of signal variance above this control value. We calculated standard deviations separately for each plate using all wells. Signals near or above this level were rare and we evaluated them as potential hits. Compounds indicated by black squares above the 5 SD level showed activity against the parental CHO cell line and were not evaluated further. Blue squares indicate compounds that had activity against both Kv12.2 and Kv12.1 in the FLIPR assay format, and green squares indicate Kv12.2–selective hits. CX4, the compound used in this study, was among the highest Kv12.2–specific signals. (**d**) Screening cascade used to identify CX4 as a specific pharmacological inhibitor of Kv12.2. Green lines indicate desired result at each stage. Primary hits from the Kv12.2 screen (64) were tested against the parental CHO line to eliminate non–channel based hits, yielding 46 potential positive compounds. 26 of these hits were selective for Kv12.2 over Kv12.1, the most closely related K^+ channel, in the FLIPR format. Five of these 26 compounds blocked Kv12.2 currents in voltage–clamped *Xenopus* oocytes at –20 mV by > 50% with a 10 μM concentration. (**e**) We tested compounds against a panel of other voltage–gated K^+ channels to further assess selectivity. CX4 remained selective for block of Kv12.2 at 10 μM (recorded at –20 mV; n = 4–6). (**f,g**) 10 μM CX4 blocks steady state Kv12.2 currents at hyperpolarized voltages by depolarizing the voltage–activation range.

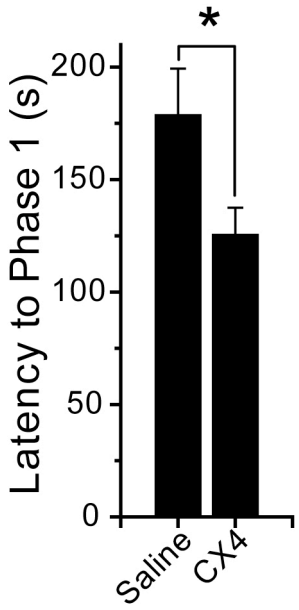

Supplementary Figure 5 | CX4 reduces latency to PTZ–induced seizure. Direct bilateral injection of CX4 into the hippocampus of *C57Bl/6J* mice significantly reduced the latency to seizure following a subsequent intraperitoneal injection of PTZ (40 mg/Kg). Latency is measured as the time in seconds to Phase 1 seizure, as described in **Fig. 3**. We used saline injections as a control; the asterisk indicates significance ($p < 0.05$; $n = 11$ each).

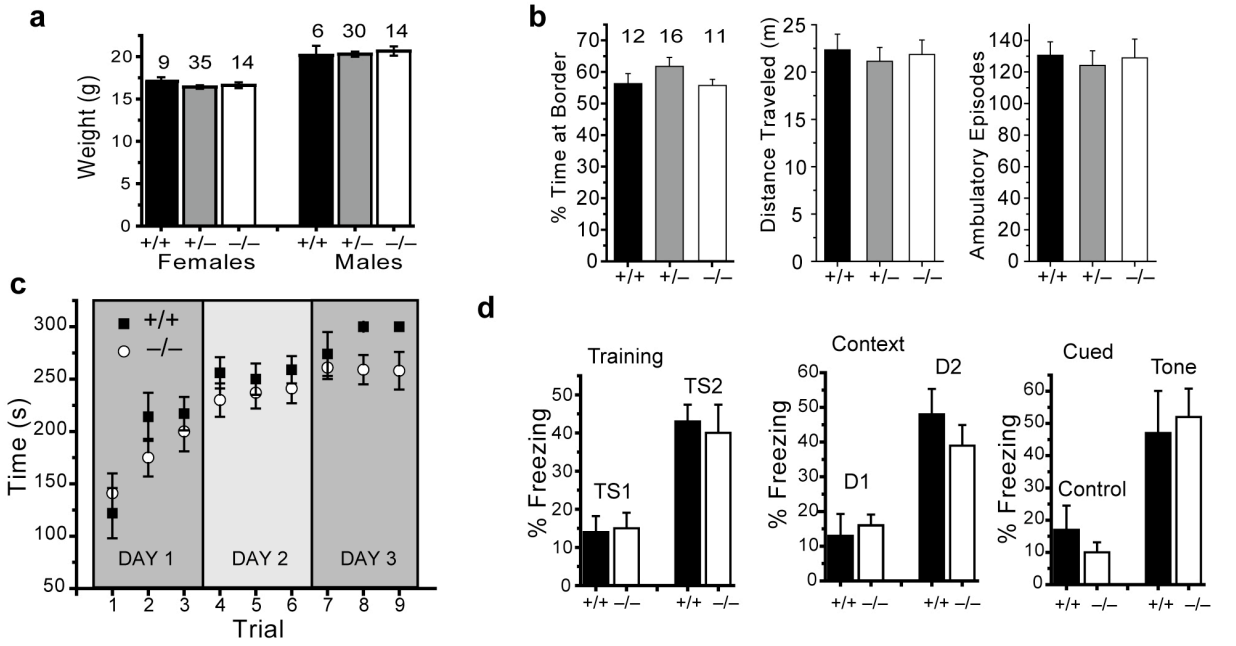

Supplementary Figure 6 | Normal Kv12.2 behavioural phenotypes. (**a**) Weights of 8–11 week old male and female *Kv12.2*$^{+/+}$, *Kv12.2*$^{+/–}$ and *Kv12.2*$^{–/–}$ mice indicated normal feeding behaviour and metabolism; *n* given above bars. (**b**) We monitored anxiety and exploratory activity using an open–field apparatus. Time spent at the border is a measure of anxiety level, whereas distance travelled and ambulatory episodes measure exploratory activity. No changes in open field behaviour were observed; *n* given above the first set of bars. (**c**) Motor coordination and memory: *Kv12.2*$^{–/–}$ mice ($n = 20$) showed normal coordination and motor learning compared to *Kv12.2*$^{+/+}$ mice ($n = 10$) in accelerated rotarod testing. Values show mean ± s.e.m. time to fall during 9 sequential rotarod trials given over 3 days. (**d**) Contextual and cued memory tested using a fear conditioning paradigm (see **Methods**). *Kv12.2*$^{+/+}$ and *Kv12.2*$^{–/–}$ mice showed a similar increase in freezing during the second tone (left), and when placed in the same chamber 24 hours later (middle, D2) in the absence of tone or shock (contextual memory). 4 hours later mice were placed in visually distinct chamber and exposed to the tone to cue freezing behaviour; both *Kv12.2*$^{+/+}$ ($n = 8$) and *Kv12.2*$^{–/–}$ ($n = 10$) mice showed robust freezing after tone presentation, indicating strong cued memory of the training (right).

Supplementary Methods

Phylogenetic analysis. We gleaned EAG channel family amino acid sequences from mouse, *Nematostella* and *Trichoplax* genome annotations and blast searches of genome assemblies[3, 4] and aligned them using Clustal W (manually adjusted as necessary). We built the phylogeny using the Minimum Evolution Distance Algorithm implemented in Mega4[5] with pair wise deletion of gaps. The phylogeny was subjected to 100 Bootstrap replications; the displayed gene family groupings were observed 100% of the time. Most of the *Nematostella* and *Trichoplax* sequences appear incomplete at the C–terminus, but contained the conserved regions useful for phylogenetic analysis. A probable fifth Kv11 family sequence from *Nematostella* was excluded from analysis because of gaps in conserved sequence. Amino acid sequences used in the analysis are included in the **Supplementary Sequences** text file.

Animals. All animal work adhered to procedural protocols approved by the IACUC committees of Baylor College of Medicine (EEG), the Genomics Institute of the Novartis Research Foundation (production of germ line chimaeras), or the Scripps Research Institute (behavioural, molecular and electrophysiological analyses).

Generation of *Kv12.2*$^{-/-}$ knockout mice. We produced and maintained the *Kv12.2*$^{-}$ and *Kv12.2*^{loxP} alleles in a pure *C57BL/6* strain background. Bruce4 ES cells[6] carrying the targeted Kv12.2 allele were injected into blastocysts from albino *C57BL/6*$^{tyrC-2J}$ mice. A single chimaeric animal demonstrated germline transmission when backcrossed to *C57BL/6*$^{tyrC-2J}$ (black coat color). We bred these offspring to *C57BL/6*$^{EIIA/Cre}$ and *C57BL/6*$^{Zp3/Flp}$ to modify Kv12.2 in the germline to produce the *Kv12.2*$^{-}$ and *Kv12.2*^{loxP} alleles, respectively. We used a PCR screen

followed by complete sequencing to confirm proper allele structure. We used a rabbit polyclonal antibody recognizing the C–terminus of the Kv12.2 channel[7] for Western blot analysis of Kv12.2 protein expression as previously described.

PCR–based genotyping of littermates. We digested mouse tail tips in 100µl lysis buffer (NaOH 25mM/EDTA 0.2 mM) at 95°C for 20 minutes, neutralized the mixture by adding 100µl Tris–HCL 40 mM, and used 1 µl of the sample in each genotyping PCR reaction (20 µl). We used Go Taq Hot Start polymerase (Promega, Madison, WI) for amplification. Primers for the $Kv12.2^{+}$ allele, 5'–CTT GGG TCC CAC CAG ACC TTT GA–3' (sense) and 5'–CGG ACG GCT TAG CTA AAA CCA AAC AA –3' (antisense), span the Neo^{R} cassette insertion site and produce a 162 bp amplicon only from the $Kv12.2^{+}$ allele. We substituted the sense primer with 5'–AGC ACC CCT CAC TCC CCA ATA CAT T–3' for $Kv12.2^{-}$ and with 5'–TGG GTC CCA CCA TTA ACC CTC ACT AA–3' for the $Kv12.2^{loxP}$. The $Kv12.2^{-}$ primer produces a 447 bp amplicon following CRE excision of exons 2–4, and the $Kv12.2^{loxP}$ primer produces a 330 bp amplicon following Flp excision of the Neo^{R} cassette. We performed 35 PCR cycles (95°C 30 seconds, 60°C 30 seconds, and 72°C 30 seconds) to produce the amplicons and gel electrophoresis was used to analyze results.

Electrophysiological recording in *Xenopus* oocytes. Preparation of *Xenopus* oocytes, production of cRNAs and voltage clamp recordings of Kv12.2 and Kv7.2/7.3 currents expressed in oocytes were performed as described previously[8, 9].

Whole cell patch clamp of cultured neurons. We dissected hippocampi in ice–cold HBSS

solution (Invitrogen, Carlsbad, CA) containing 20% fetal bovine serum (HyClone, Logan, UT), cut them into 1 mm cubes and digested them with papain (Worthington, Lakewood, NJ) for 45 min. We mechanically dissociated neurons in HBSS supplemented with 12 mM $MgSO_4$ using fire–polished Pasteur pipettes, centrifuged this cell suspension at 1000 rpm for 5 min and plated neurons onto coverslips coated with rat collagen (Millipore, Billerica, MA) and poly–L–lysine (Invitrogen, Carlsbad, CA) in MEM supplied with B–27, Ara–C and transferrin. Cells were incubated in 24–well plates at 37ºC and 5% CO_2.

We performed whole–cell patch–clamp recordings on pyramidal neurones (identified by shape) after 8–10 days of culture at room temperature. Neurons were continuously perfused during recording with an extracellular solution containing (in mM): 140 NaCl, 4 KCl, 1 $MgCl_2$, 2 $CaCl_2$, 10 HEPES, 10 glucose, adjusted to pH 7.4 with NaOH and to 290 mOsm with sucrose. Recording pipettes pulled from borosilicate glass had tip resistances of 3 – 5 MΩ when filled with intracellular solution (in mM: 120 K–gluconate, 15 KCl, 1 $MgCl_2$, 5 HEPES, 5 EGTA, 2 Mg–ATP, pH 7.4, 290 mOsm). For voltage–clamp recordings of K^+ currents, TTX (1μM), D,L–AP5 (100 μM), CNQX (50 μM) and picrotoxin (50 μM) were added to the external solution to block voltage–gated sodium currents, ionotropic glutamate receptors and GABA–A receptors, respectively. We used an Axopatch 200B amplifier and the pCLAMP acquisition suite (Molecular Devices, Sunnyvale, CA) for patch clamp recording. Cell capacitance and series resistance were compensated, data were low–pass filtered at 2 kHz, digitized at 5 kHz and analyzed using pCLAMP and Origin 7.5 (OriginLab, Northampton, MA). To measure the threshold for action potential firing, we plotted the time derivative of membrane potential (dV/dt) against membrane potential, defining threshold as the point at which dV/dt increased abruptly [10].

Hippocampal Slice Recording. We obtained slice recordings from horizontal hippocampal slices taken from *Kv12.2*$^{+/+}$ and *Kv12.2*$^{-/-}$ mice aged 8 to 9 weeks. We removed brains from isofluorane–anesthetized mice, placed them in ice–cold, equilibrated (95% O_2 and 5% CO_2) cutting solution (in mM: 246 sucrose, 2 KCl, 1.25 NaH_2PO_4, 26 $NaHCO_3$, 10 glucose, 2 $MgSO_4$, 0.5 $CaCl_2$, and 1 Na^+ L–ascorbate) and cut 350 μm thick slices with a vibratome (Leica). Slices recovered in equilibrated (95% O_2 and 5% CO_2) ACSF recording solution (in mM: 124 NaCl, 3 KCl, 1.25 NaH_2PO_4, 26 $NaHCO_3$, 10 glucose, 1.5 $MgCl_2$, 2.5 $CaCl_2$) at room temperature for at least 1 hr before recording. We perfused slices with equilibrated ACSF supplemented with 100 μM picrotoxin, 50 μM AP–5 and 100 μM CNQX at 2 ml/min to block major synaptic inputs during recording. We identified CA1 neurones visually using DIC video and performed whole–cell patch clamp experiments at room temperature 1 to 6 hr after slices were cut using 3–5 MΩ pipettes filled with an internal solution containing (in mM): 120 K–gluconate, 15 KCl, 1 $MgCl_2$, 5 HEPES, 5 EGTA, 2 Mg–ATP, pH 7.4, 290 mOsm.

Lentivirus production. We produced lentivirus by transfecting host cells (HEK293t) with VSVg, CMVΔ8.9 and pFUGW as described by Ho et al., 2006[11]. VSVg and CMVΔ8.9 encode the elements of viral envelope and pFUGW is a shuttle vector which carries the CRE–GFP fusion protein and encodes genes required for viral replication. We harvested media containing lentivirus 48 hours post–transfection and passed it through a 0.45 μm filter to remove cell debris. We infected neurons with 150–250 μl of viral supernatant/well in 24–well plates 1 day post culture and incubated them for 7–10 days to allow for Cre expression. Close to 100% of neurons in the cultures labelled with GFP using this procedure.

Video–EEG recording and PTZ testing. We performed EEG recordings as previously described[12]. Briefly, we implanted teflon–coated silver wire electrodes (0.005 inch diameter) bilaterally into the subdural space over frontal, temporal, and parietal cortices of adult littermates (4–5 months) under anaesthesia. We monitored digital EEG activity and behaviour of freely moving mice daily for up to two weeks at random intervals. For PTZ experiments, we injected mice intraperitoneally with 40 or 50 mg/kg of PTZ in 0.9% NaCl; we classified convulsive seizures developing after injections into phases as described previously[13].

***In vivo* hippocampal administration of the Kv12.2 inhibitor.** For PTZ experiments involving CX4 administration, we cannulated 3–5 month old *C57Bl/6J* animals using stereotaxic coordinates and methods described by Stiedl et al. (2000)[14] for direct hippocampal injection. Briefly, we implanted bilateral guide cannulae (Plastics One, C235GS–5–2.0/SPC, 0.46 mm outer diameter, 2 mm C/C distance) 1.5mm into the brain past the skull surface. We fixed the cannulae using superglue, dental cement and a screw, and sutured incisions. Mice recovered for at least two days prior to CX4 injections. We used injection cannulae (Plastics One, C235IS–5/SPC) inserted 1 mm past the guide cannulae to bilaterally apply 0.75 μl of the Kv12.2 inhibitor CX4 (50 μM) or vehicle. We used isoflurane to anesthetize mice during surgery and injection, and kept them under a continuous regimen of the analgesic and anti–inflammatory drug flunixin (s.c., 0.1 ml per 10g body weight at 0.25 mg/ml) until injection day.

Behavioural experiments. We monitored anxiety and exploratory activity using an open–field apparatus consisting of a square (43 x 43 cm) acrylic box equipped with 16 movement sensors on each side, plus vertical movement sensors (Med Associates Inc., St. Albans, VT). We observed individual mice placed in the test chamber for 20 min, during which the distance travelled,

ambulatory episodes, and time spent at the borders (within 10 cm of the arena edge) were recorded. Time spent at the border measures anxiety level, whereas distance travelled and ambulatory episodes measure exploratory activity.

We assessed motor coordination and memory of *Kv12.2*$^{-/-}$ mice using an accelerating rotarod apparatus (Ugo Basile, Italy). Coordination was tested by placing mice on a rod and accelerating its rotation evenly from 4 to 40 rpm over a 5 min interval. We scored mice for time to fall in 3 tests separated by 30 min rest intervals; tests were repeated on three consecutive days to assess motor learning.

We tested contextual and cued memory using a fear conditioning paradigm in which fear (freezing behaviour) of a shock is measured. We trained mice by placing them in a chamber with visual cues (CL–M2; O'Hara, Tokyo, Japan) for 3 min and then presenting them with two tone (85 dB, 2800 Hz, 20 s)/foot shock (0.5 mA, 2s) pairs (TS1 and TS2). We measured contextual and cued memory separately using the chamber environment and the tone, respectively, as described in **Supplementary Fig. 6**.

Statistics. We assessed the significance of differences between pairs of mean values using two–sample *t*–tests. *P* values < 0.05 are reported as significantly different.

Supplementary References

1. Gutman, G.A.*, et al. Pharmacol Rev* **55**, 583–586 (2003).
2. Zhang, J.H., Chung, T.D. & Oldenburg, K.R. *J Biomol Screen* **4**, 67–73 (1999).
3. Putnam, N.H.*, et al. Science* **317**, 86–94 (2007).
4. Srivastava, M.*, et al. Nature* **454**, 955–960 (2008).
5. Tamura, K., Dudley, J., Nei, M. & Kumar, S. *Mol Biol Evol* **24**, 1596–1599 (2007).
6. Kontgen, F., Suss, G., Stewart, C., Steinmetz, M. & Bluethmann, H. *Int Immunol* **5**, 957–964 (1993).
7. Clancy, S.M., Chen, B., Bertaso, F., Mamet, J. & Jegla, T. *PLoS One* **4**, e6330 (2009).
8. Jegla, T. & Salkoff, L. *J Neurosci* **17**, 32–44 (1997).
9. Zhang, X.*, et al. Biophys J* **97**, 110–120 (2009).
10. Bean, B.P. *Nat Rev Neurosci* **8**, 451–465 (2007).
11. Ho, A.*, et al. J Neurosci* **26**, 13089–13101 (2006).
12. Glasscock, E., Qian, J., Yoo, J.W. & Noebels, J.L. *Nat Neurosci* **10**, 1554–1558 (2007).
13. Weiergraber, M.*, et al. Epilepsia* **47**, 839–850 (2006).
14. Stiedl, O., Birkenfeld, K., Palve, M. & Spiess, J. *Behavioural brain research* **116**, 157–168 (2000).